

J. ZIMMERMAN\*

## FINITE ELEMENT MODELLING OF THE RESIDUAL STRESSES INDUCED IN THERMALLY DEPOSITED COATINGS

### MODELOWANIE METODĄ ELEMENTÓW SKOŃCZONYCH NAPRĘŻEŃ WŁASNYCH POWSTAJĄCYCH W PROCESACH TERMICZNEGO NANOSZENIA POWŁOK

A numerical model based on the finite element method has been constructed with the aim to examine the residual stress state induced during thermal deposition of coatings on various substrates. The first stage of the modelling was designed to solve the problem of the high-velocity impact of a single spherical particle on a substrate using the “dynamics-explicit” module of the FEM ADINA software. In the second stage, the deposition process was simulated as a progressive growth of the coating until it achieved the desired thickness, and then the entire system was cooled to the ambient temperature. This problem was assumed to be thermo-mechanical and was also solved with the use of the FEM ADINA software. The samples assumed in the computations were cylindrical in shape and were built of a titanium coating, with three different thicknesses, deposited on an  $Al_2O_3$  ceramic substrate by the detonation method. The numerical model was verified experimentally by measuring the deflection of the samples after their cooling. The computed values appeared to be in good agreement with those obtained experimentally.

*Keywords:* coatings, thermal spraying, residual stress, finite element modelling

Opracowano numeryczny model obliczeniowy z użyciem metody elementów skończonych do określania naprężeń własnych powstających w procesach termicznego nakładania powłok na podłoża. W pierwszej fazie modelowania rozwiązano na przestrzennym modelu zagadnienie uderzenia pojedynczych kulistych cząstek z dużą prędkością w podłoże, wykorzystując moduł „dynamics-explicit” programu FEM „ADINA 8.6”. W drugiej statycznej fazie modelowania przeprowadzono symulację procesu poprzez przyrostowe budowanie powłoki, aż do uzyskania określonej grubości, a następnie schłodzenie całego układu. Zagadnienie drugiego etapu rozwiązano, jako termomechaniczne, przy użyciu programu FEM software ADINA 8.6. Obliczenia przeprowadzono dla walcowych próbek składających się z tytanowej powłoki o trzech grubościach naniesionej na podłoże ceramiczne  $Al_2O_3$  metodą detonacyjną z prędkością uderzenia 800m/s. Model obliczeniowy został zweryfikowany eksperymentalnie przez pomiary ugięcia próbek po ich schłodzeniu. Otrzymano dobrą zgodność wyników obliczeń numerycznych ugięć układu powłoka/podłoże z wartościami doświadczalnymi.

## 1. Introduction

Methods of thermal deposition of coating materials on the surfaces of various products permit depositing metallic, ceramic, and composite layers as well as functionally graded coatings on metallic and ceramic substrates. Such a great variety of materials suitable for treating by these methods permits producing the coating/substrate systems with the desired performance properties such as good resistance to frictional wear, corrosion, erosion, and provides possible solution to counter the problem of hot corrosion in high temperature environment [1].

The idea underlying the thermal deposition methods consists in the ejection of the coating material powder with high velocity towards the substrate. The spherical particles impinging upon the substrate surface undergo considerable deformation (are flattened), are clamped within the surface inequalities and adjust their shapes to them, and finally join with the

next particles that hit the substrate thereby forming a coating with a desired thickness [2 - 4]. Then the entire system is cooled to room temperature. The high kinetic and thermal energies involved in the process, the substantial differences in temperature between the substrate and the consecutive layers of the coating, and also the considerable mismatch between the properties of the materials being joined result in residual thermal stresses being induced in the coating/substrate system. As demonstrated by investigators [5], the residual stresses can degrade the mechanical strength of the coating, may lead to delamination and thereby shorten the service life of the operating surface of the coating. The estimation of the magnitude of the residual stresses active in the coating/substrate systems is therefore an essential problem to be solved.

Examination of the magnitude of residual stresses induced in thin layers is difficult and expensive. There are several methods used for the determination of residual stress profiles generated in coating/substrate systems. The mostly known and

\* WARSAW UNIVERSITY OF TECHNOLOGY, FACULTY OF PRODUCTION ENGINEERING, 85 NARBUTTA STR., 02-524 WARSAW, POLAND

used are neutron diffraction method [6, 7], X-ray diffraction technique [8, 9], layer removal method [7] or hole-drilling method [3]. Each of them has its own advantages and disadvantages therefore there is no one favored method that can be used for testing all kind of coating materials.

Many investigators examined the residual stresses induced in thermally deposited coatings using analytical methods, but they usually focused on uncomplicated systems and did not take into account the plastic behavior of the metallic materials [3, 10].

There are numerous literature reports devoted to the numerical modeling of the residual stress state induced in coating/substrate systems, often utilizing the finite element method. Certain investigators examined axisymmetric models, coatings formed as a single layer with the load imposed on the mechanical model being the time-varying temperature field [11-15]. Other numerical models were based on the assumption that the coating grows through the successive activation of the consecutive layers of the material being deposited [2, 16-19].

Many investigators attempted at modelling the residual stresses induced during thermal deposition of coatings on various substrates but they did not take into account the effect of the mechanical stresses induced when a particle of the coating material impinges onto the substrate. The present study considers this problem. The residual stress distributions were determined using the example of a titanium coating, with three different thicknesses, deposited on an  $\text{Al}_2\text{O}_3$  ceramic substrate by the detonation method. This coating may be used for metallization of ceramics or as an intermediary layer which enables ceramics to be joined with various metals [20, 21]. The calculated values of the deflections of the coating/substrate system were compared with values obtained experimentally.

## 2. Process description

In thermal spraying of metals on ceramic substrates, very good results are obtained when spraying is realized by the detonation method. That was verified by the research [15, 21] in which pure titanium was thermally sprayed by the detonation gun technique onto the  $\text{Al}_2\text{O}_3$  and  $\text{AlN}$  ceramic substrates.

The titanium coatings, 0.1 mm, 0.145 mm, and 0.22 mm thick, were deposited on an  $\text{Al}_2\text{O}_3$  substrate shaped as a disk 27 mm in diameter and 0.65 mm thick. The coating material was pure titanium (99.7%) in the form of a powder with a particle diameter of 40-50 $\mu\text{m}$ . The detonation gun employed was 1000 mm long, 25 mm in diameter, and was operated in valveless mode. The parameters of the detonation spraying process are given in Table 1.

During each 'shot' the coating material particles hit the substrate (at a velocity about 800 m/s) and were 'anchored' on its surface covering an area with a diameter of 30-35 mm. The thickness of the coating obtained after one shot was about 0.05 mm. Thanks to the high kinetic energy of the particles shot towards the substrate, the coating obtained has a homogeneous, densely packed, multi-layer structure. Fig.1 shows the microstructure of a Ti coating, about 0.145 mm thick, deposited on an  $\text{Al}_2\text{O}_3$  substrate. The coating adhered well to the substrate and was little porous.

TABLE 1  
Process parameters in the detonation spraying of the Ti coating on an  $\text{Al}_2\text{O}_3$  substrate [21]

Detonation mixture pressure (MPa)		Purge gas pressure (MPa)	Detonation frequency (Hz)	Nozzle distance from the substrate (mm)
propane 0.08	oxygen 0.12	nitrogen 0.08	10	160

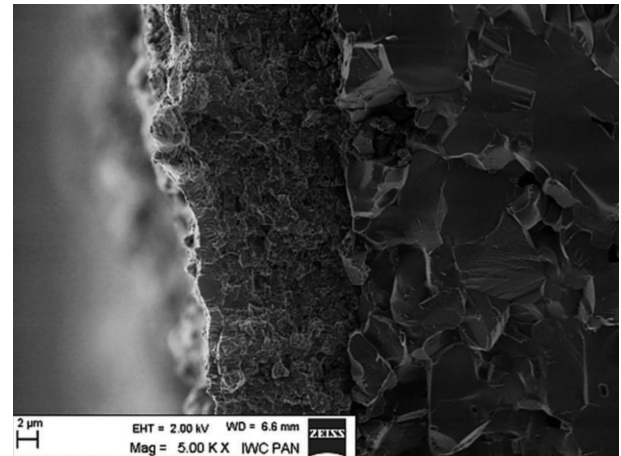


Fig. 1. Microstructure of a Ti coating deposited on an  $\text{Al}_2\text{O}_3$  substrate by the detonation method [21]

## 3. Methodology adopted in the modeling of residual stresses induced in thermally deposited coatings

The thermal deposition process has the two principal stages. The first stage includes high-velocity dynamic impacts of the coating material particles on the substrate and on the previously deposited sub-layer, and the next stage is the deposition process of the coating material on the substrate. The processes of the thermal-deposition of coatings are complex and their course depends on many factors such as the size, temperature and shape of the coating particles, their impact velocity, the required final thickness of the coating, the kind of the bonded materials, the condition of the substrate surface, and the technique of cooling. In view of this complexity, certain simplifying assumptions were introduced in its physical course, which permitted constructing a numerical model which computed the residual stresses using the finite element method. The adopted assumptions include:

- The impact of the high-velocity particles onto the substrate results in their substantial deformation, with 80% of the kinetic energy being transformed into deformation energy and heat energy. The particles are flattened and thin sub-layers are formed. The subsequent sub-layers are deposited after each detonation cycle.
- The time interval during which the particles are in the impact zone and are heated and cooled down is shorter than the time interval between the consecutive detonation impacts. The next impinging particles are deposited on the previously formed sub-layer which is already solidified. This assumption [22] de-couples the problem of fluid dynamics and permits reducing the problem to

thermo-mechanical one. The substrate and the sub-layers are modeled in the solid state with a specified temperature field, and the mechanical and physical properties of the materials depend on the temperature.

- The sub-layers formed during one cycle are arranged in parallel to one another.
- The substrate and the subsequent sub-layers are assumed to be in ideal contact which means that they fully adhere to each other and there is no heat barrier between them.

The thermal deposition process was modeled in two phases. The first phase included the solution of the problem of the impact of spherical Ti powder particles on the ceramic substrate and on the previously deposited sub-layer. Some values obtained in this modelling phase were introduced as the boundary conditions into the next modelling phase. This phase was to solve the static problem of building the coating in the form of progressively growing platelets until it acquires the desired thickness, and then cooling the entire system obtained to room temperature. Fig. 2 shows schematically the method used for determining the final distribution of residual stresses in the coating/substrate system.

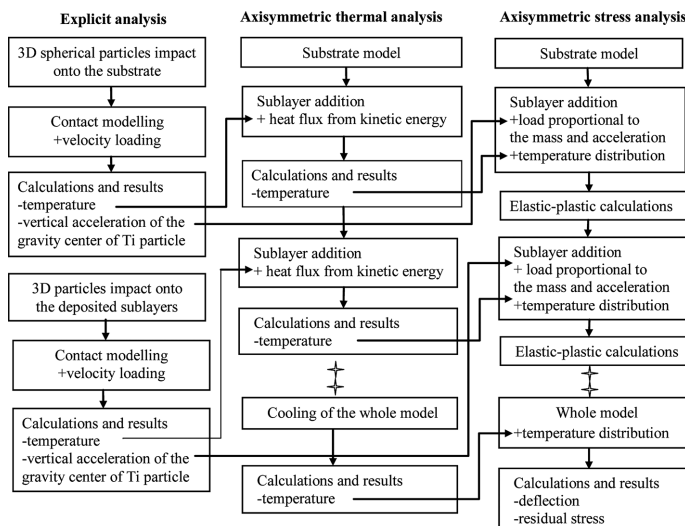


Fig. 2. Flow chart of the method used for determining the residual stress distribution in thermally sprayed coatings

### 3.1. Modeling the particles impact

Literature review [4] shows that, during the flight, the powder particles do not coagulate so that each particle can be considered individually and separately from the other particles. Therefore, it is the impact of the individual coating particles on the substrate which is modelled. The modelling of the particles movement dynamics was based on the simplifying assumption that the spherical particles 0.05 mm in diameter have the same velocities, perpendicular to the substrate, and that they hit the substrate at the same time at a velocity of 800 m/s forming a hexagonal configuration, which ensures the maximum packing. The solution utilized the symmetry planes which permitted reducing the size of the problem. The contact planes, appropriately situated in the model, block the subsequent particle rows. Fig. 3 shows the adopted geometry of the segment together with the displacement-blocking plates and the FEM mesh. The bold lines indicate the con-

tact surfaces (10 pairs in total). The numerical calculations were performed using the FEM-ADINA Dynamics Explicit software. The titanium properties adopted in the calculations were: density= 4540 kgm<sup>-3</sup>, elastic-plastic model with the Young modulus=129.04GPa, Yield stress=500MPa, tangent modulus=500MPa. The Al<sub>2</sub>O<sub>3</sub> substrate was modeled as an elastic material with density=3900 kgm<sup>-3</sup>, and the Young modulus=318.2GPa.

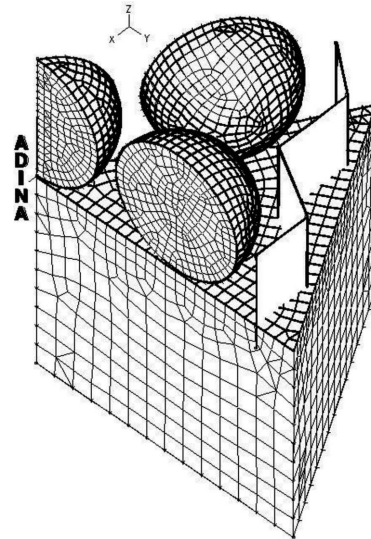


Fig. 3. FEM mesh used in the model representing the impact of spherical Ti particles on an Al<sub>2</sub>O<sub>3</sub> substrate

### 3.2. Thermo-mechanical model

In modelling the process of thermal deposition of the coating material on the substrate it was assumed that both elements were cylindrical in shape. The modelling of the temperature field was divided into several stages in which the computations were based on the transient heat transfer equations. It was assumed that after each particle impact, a new sublayer appeared, with the thickness 'g<sub>c1</sub>', and this was repeated at the time intervals 't<sub>1</sub>' dependent on the spraying frequency. The first sublayer of the coating material with the temperature 'T<sub>c1</sub>' appears after the prescribed short time interval 't<sub>0</sub>'. The interface between this sublayer and the substrate is loaded with the heat flux 'q' active during the time 't<sub>z</sub>'. The flux 'q' was chosen so as to ensure the temperature increase by 430°C that results from the transformation of the kinetic energy into heat energy at the assumed spraying rate of 800 m/s. The upper surface of sublayer is heated by the heat source which involves the ambience with the temperature 'T<sub>b</sub>' and heat exchange through the convection 'h<sub>b</sub>' resulted by the draught from the moving particles.

The first stage is completed after the time 't<sub>1</sub>' when the next sublayer with the temperature 'T<sub>c2</sub>' appears. The interface between these two sublayers is loaded with the heat flux 'q' for the time 't<sub>z</sub>' just as was the case in the previous cycle. The process is repeated until the coating acquires the specified thickness. In the final stage the entire system is cooled to the ambient temperature.

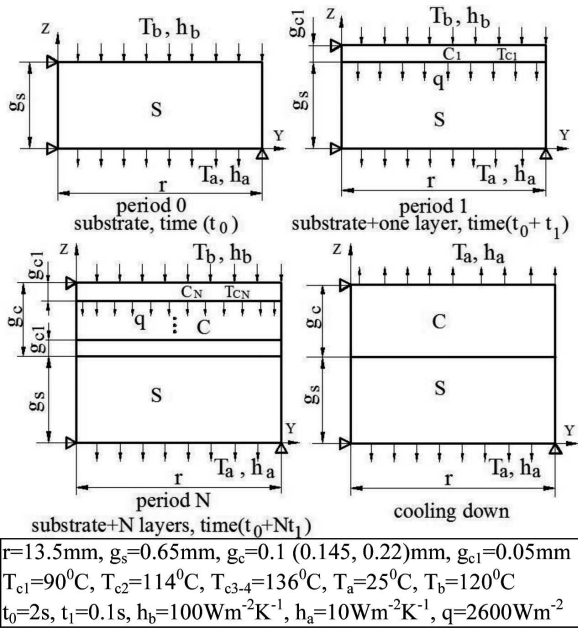


Fig. 4. Description of the boundary conditions with the up-dated geometry of the model for determining the temperature field in thermally sprayed coatings (data assumed in the computations are given in the inset)

Figure 4 shows the up-dated geometry of the model together with the initial and boundary conditions assumed in the analysis. The solution of the temperature field was obtained using the thermal model of the FEM ADINA software. The elements used in the computations were 4-node axisymmetric conductive elements for the substrate and coating materials, and 2-node convection elements at the boundaries. The conductive elements of the newly deposited sublayer and the convection elements of its upper surface are activated at the time intervals ‘t<sub>1</sub>’, whereas the convection elements in-between the sublayers are deactivated. Therefore the modelling of the temperature field is here the problem with moving boundary conditions in which the outer surface of the coating grows at the time intervals dependent on the spraying frequency.

The temperature field is a factor that activates thermally the process of mechanical deformation. Depending on the magnitude of temperature gradients some parts of titanium coating may undergo plastic deformations, which may relax the residual stresses in the final coating. The load in the stress analysis is thus the known temperature field obtained from the solution of the transient heat transfer during the successive time increments, with activated newly-deposited sublayers, which is superposed on the mechanical field in the ‘time steps’ series. The modelling of residual stresses also included the effect of the impacts of the individual coating powder particles on the substrate and on the previously deposited sublayer. This was realized by assuming that the load is proportional to the mass and acceleration (active in a short time of 0.1μs) of each newly deposited sublayer. The magnitude of this acceleration was estimated based on the deformation-time variation of the mass center of the centrally-situated spherical Ti particle, obtained from the solution of the particle impact dynamic problem.

The behavior of the ceramic substrate material was described by an elastic model, and the coating material - by an elastic-plastic model. Tables 2 and 3 give the thermomechan-

ical properties of the materials of the Ti coating and Al<sub>2</sub>O<sub>3</sub> substrate (in dependence on the temperature).

TABLE 2  
Thermomechanical properties of Ti, assumed in the calculations [23]

Temperature(°C)	27	127	227	327	427	527	627
Specific heat(Jkg <sup>-1</sup> K <sup>-1</sup> )	523	546	561	597	632	672	700
Thermal conductivity (Wm <sup>-1</sup> K <sup>-1</sup> )	21.9	21.0	20.4	19.7	19.4	19.7	20.7
Young’s modulus (GPa)	129.8	128.8	126.8	123.8	120	115	109
Yield strength (MPa)	500	453	326	233	170	122	86
Thermal expansion coefficient·10 <sup>-6</sup> (K <sup>-1</sup> )	8.4	8.7	9.1	9.4	9.7	9.9	10

TABLE 3  
Thermomechanical properties of Al<sub>2</sub>O<sub>3</sub>, assumed in the calculations [24]

Temperature(°C)	27	127	227	327	427	527	627
Specific heat (Jkg <sup>-1</sup> K <sup>-1</sup> )	754	951	1005	1089	1130	1151	1172
Thermal conductivity (Wm <sup>-1</sup> K <sup>-1</sup> )	34.6	25.1	19.0	14.7	11.2	9.5	8.6
Young’s modulus (GPa)	318.3	316.9	315.3	313.2	310.5	307.3	303.6
Thermal expansion coefficient·10 <sup>-6</sup> (K <sup>-1</sup> )	5.9	6.5	7.1	7.6	8.0	8.4	8.7

#### 4. Computation results

##### 4.1. Particle impact on the substrate and the previously-deposited sublayer

Figure 5 illustrates the deformation of the spherical Ti particle geometry after its impingement on the Al<sub>2</sub>O<sub>3</sub> ceramic substrate superposed on the deformed FEM mesh, and the equivalent plastic strain of the Ti particles. We can see that the particles are flattened, their neighboring surfaces are in contact, and the space between the individual particles is filled, which indicates that the coating sublayer obtained as a shape of splat. The magnitude the titanium particles are flattened on the surface reaches 50% of their initial size (from 0.05 mm diameter to 0.025 mm height).

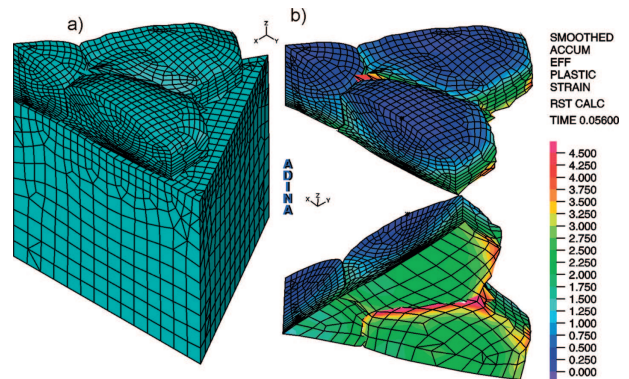


Fig. 5. Deformation of the spherical Ti particles after their impact on an Al<sub>2</sub>O<sub>3</sub> ceramic coating (a), equivalent plastic strain of the Ti particles (b)

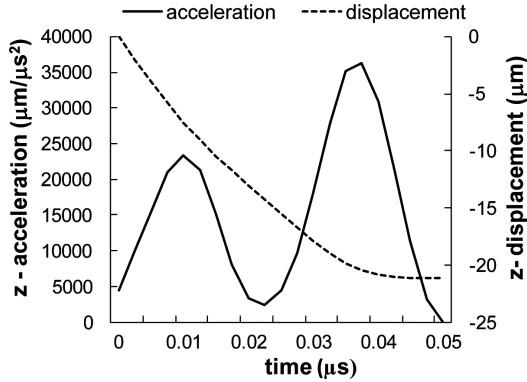


Fig. 6. FEM-calculated vertical displacement and acceleration of the mass center of the centrally-positioned Ti particle after its impact onto the  $\text{Al}_2\text{O}_3$  substrate

Fig.6 shows the computed variations of the displacement and acceleration of the mass center of the centrally-situated spherical Ti particle. The visible oscillations of acceleration result from numerical differentiation procedures. Also, the detailed observation of the displacement curve allows finding inflection points. This is probably the effect of dynamic response of titanium particle impacting onto ceramic/titanium substrate. It is observed in a very short time in the first 0.05  $\mu\text{s}$  from the impact.

The deformed geometry of the model after Ti particles impinges on the previously deposited uniform Ti sublayer, and the equivalent plastic strain of the two elements can be seen in Fig. 7. In this case the impinging particles go dip into the preceding Ti sublayers. The spherical particles are also flattened (by 40%) and anchored in the deformed Ti sublayer.

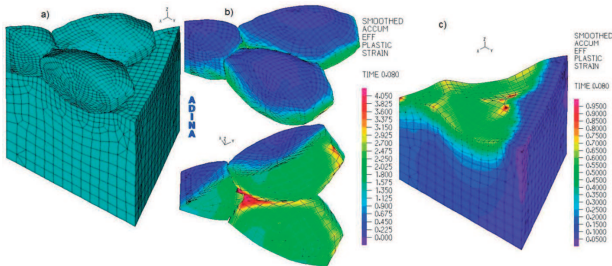


Fig. 7. Deformation (a) and equivalent plastic strain distribution of spherical Ti particles (b) after their impact into the previously deposited Ti sublayers (c)

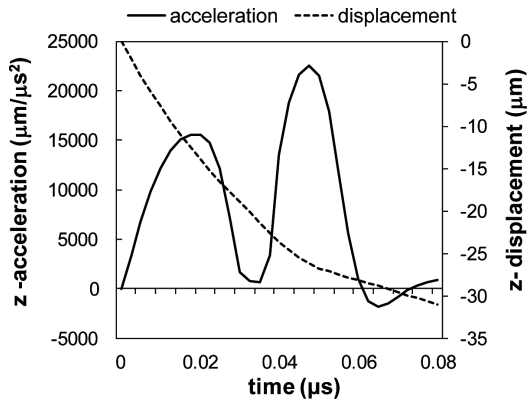


Fig. 8. FEM-calculated vertical displacement and acceleration of the mass center of the centrally-positioned Ti particle after its impact onto a Ti sublayer

The variation of the vertical displacement and acceleration of the mass center of the centrally-situated spherical particle as a function of time after its impact onto a Ti sublayer is shown in Fig.8. Upon the impact of the particle on the  $\text{Al}_2\text{O}_3$  ceramic substrate, the acceleration due to particle deformation in time reaches a value of  $-35200 \mu\text{m}/\mu\text{s}^2$ . When the particle impinges on the elastic-plastic Ti sublayer the acceleration is lower and amounts to  $-22500 \mu\text{m}/\mu\text{s}^2$ .

**4.2. Temperature distribution**

Figure 9 shows the calculated temperature distribution determined in the Ti coating- $\text{Al}_2\text{O}_3$  substrate system during the spraying process. The temperature profiles were drawn at the characteristic points positioned along the sample axis. The coating was built of five sublayers and its total thickness was 0.22 mm. As a result of the impact of the Ti particles, the temperature in the regions near the coating/substrate and sublayer/sublayer interfaces violently increases in a very short time. After the impact, the temperature of the entire system is quickly equalized until the next sublayer is formed. The rapid temperature rises and falls are characteristic of the thermal deposition processes since the coating is here deposited in a discrete way. During the entire cycle, the ceramic substrate is only slightly heated and, after the cycle is completed, it reaches a temperature of about  $80^\circ\text{C}$ .

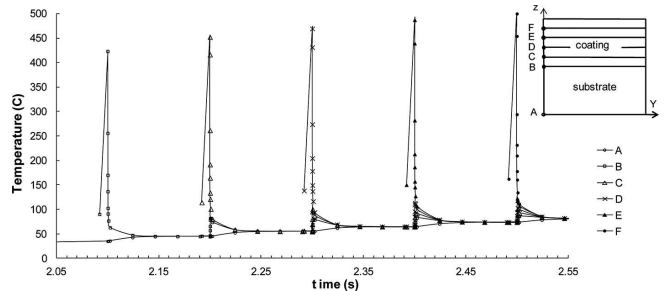


Fig. 9. FEM-calculated temperature distribution versus time at the characteristic points along the axis of the coating/substrate system

**4.3. Distribution of the residual stresses generated in the coating/substrate system**

The computed distributions of the residual stresses generated during the detonation spraying of a Ti coating on an  $\text{Al}_2\text{O}_3$  substrate, in the state after the system has been cooled down, are shown in the figures below. Figure 10 shows the bands of the radial residual stresses active in a fragment of the sample (coating thicknesses 0.145 mm). The stress distributions are uniform along the radius, except the interface near the outer cylindrical surface of the sample where their concentration is increased due to the singularity of the stress field at the edge of the system which is a typical behavior found in the FEM analysis of ceramic-metal joints [26,27]. The concentration of the radial stresses at the edge of titanium/ $\text{Al}_2\text{O}_3$  joint is probably the result of stress singularity effect that is found in FEM modeling of thermal stresses in bonded materials having different thermal and physical properties. The magnitude of the stresses in this area should not be treated quantitatively. The stress concentration suggests that the boundary of ceramic-metal interface is very important region where the coating may start to delaminate from the substrate.



Fig. 10. Radial residual stress bands determined in a fragment of the coating/substrate system (Ti coating thickness 0.145 mm)

Fig. 11 shows the profiles of the radial stress active along the sample axis as a function of the distance from the coating/substrate interface, obtained for 3 samples differing in the coating thickness. In the vicinity of point A (Fig. 9) the radial stresses are tensile (they amount to 15 MPa in the 0.1 mm coating and 40MPa in the 0.22 mm coating) and change the sign into negative at a distance of about 0.38 mm from the interface. Near the very narrow interface (about 8 $\mu$ m wide) in the region situated on the side of the ceramic substrate, the radial stresses rapidly change their sign into positive reaching a maximum of 90 MPa in the 0.1 mm-thick coating and 65 MPa in the 0.22 mm coating. On the Ti coating side, the radial stresses are negative. The stress concentration is observed at the interface. Here, the stress amplitude is approximately 150 MPa and it does not depend on the coating thickness.

In the Ti coating, the sign of the residual stresses changes with increasing distance from the interface. The maximum magnitude of the tensile stress increases with increasing coating thickness to reach about 200 MPa in the sample with the 0.22 mm-thick coating.

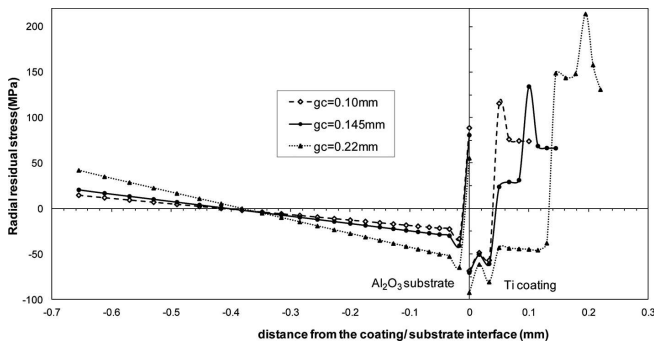


Fig. 11. Radial residual stress profiles along the sample axis as a function of the distance from the Ti-Al<sub>2</sub>O<sub>3</sub> interface for three samples with various Ti coating thicknesses (0.1 mm, 0.145 mm, 0.22 mm)

The correctness of the numerical model was verified by measuring deflections [25] of the Ti/Al<sub>2</sub>O<sub>3</sub> system produced by the detonation method. The deflection was measured at the center of the sample after each coating deposition using digital dial gauge fixed in a special stand. The indication of the dial gauge was calibrated to zero for each ceramic substrate before the coating deposition. Fig. 12 shows the deflection lines computed by the finite element method in 3 samples with differing coating thicknesses and the values of the deflection of the real objects measured in their central points. The computed and

experimental values coincide within the measurement error. The agreement is better in the samples with thinner coatings.

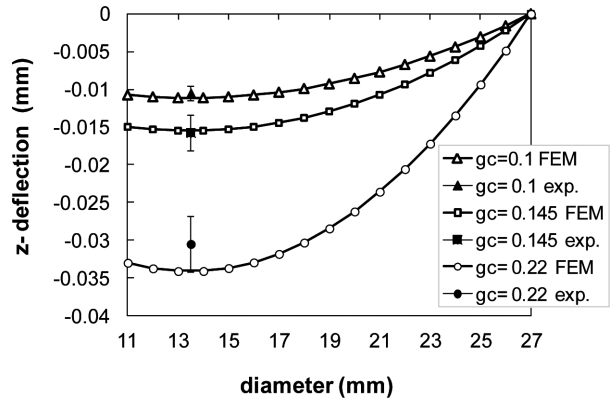


Fig. 12. Deflection of the Ti/Al<sub>2</sub>O<sub>3</sub> system calculated by FEM and measured experimentally for three differing thicknesses of the coating

Another analysis included examining the effect of pre-heating the substrate on the magnitude and distribution of the residual stresses. Fig. 13 compares the radial residual stress profiles obtained in the samples with preheated and non-heated substrates. With the substrate heated to a temperature of 80°C the residual stress level, measured after the system was cooled, appeared to be lower. Moreover, the radial stress distribution in the near-interface region was more advantageous in that the stresses were negative on both the AlO<sub>3</sub> and Ti sides. These results should be also verified by experimental methods.

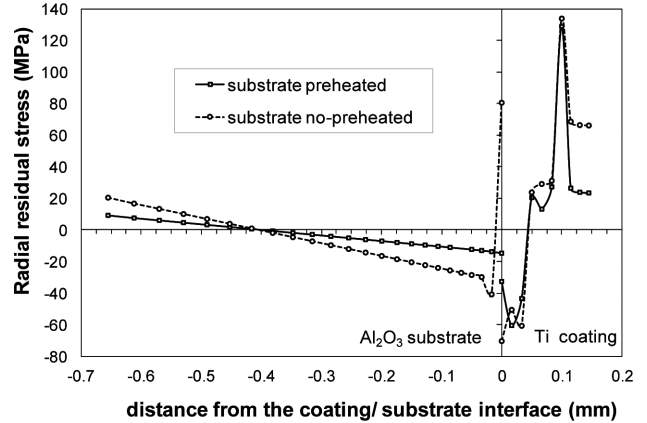


Fig. 13. Comparison of the radial residual stress profiles in the Ti/Al<sub>2</sub>O<sub>3</sub> system with the substrate preheated to T<sub>s</sub> =80°C and a non-heated substrate (Ti coating thickness 0.145 mm)

### 5. Conclusions

A new computational model based on the finite element method was constructed with the aim to anticipate the residual stress state induced during the thermal spraying of coatings on a substrate and active in the coating/substrate system after it is cooled to the ambient temperature. The modeling was performed in two stages. The first, dynamic stage was designed to solve the problem of the impact of coating material particles on the substrate and on the previously deposited sublayer using the ADINA “Dynamics-Explicit” software. In the next static stage, the coating geometry was built progressively, layer-by-layer, at the time intervals dependent on

the spraying frequency. The temperature distributions computed for the preceding sublayer were assumed to be the load imposed on the geometry of the mechanical model together with the newly-deposited sublayer. The mechanical model takes also into account the effect of a high-velocity impact of the spherical powder particles on the stress state induced in the entire system. This was realized by assuming that the load is proportional to the mass and acceleration of the newly formed sublayer particles. The acceleration was estimated based on the deformation-time variation of the mass center of the centrally-positioned spherical coating particle, which was obtained in the solution of the dynamic problem of the particle impact.

The proposed model was used for analyzing residual stresses induced in the Ti coatings, with three differing thicknesses, deposited on an Al<sub>2</sub>O<sub>3</sub> ceramic substrate by the detonation method.

The performed research allowed the formation of the following conclusions:

- after the Ti particles impact onto the Al<sub>2</sub>O<sub>3</sub> substrate, they were flattened by 50%, whereas the particles impinged on a Ti sublayer were flattened by 40%,
- upon the impact of Ti particles onto the Al<sub>2</sub>O<sub>3</sub> substrate with a velocity of 800 m/s, the acceleration of the Ti particles due to their deformation in time is of the order of  $-38000 \mu\text{m}/\mu\text{s}^2$ , whereas for the particles impinge on a Ti sublayer the acceleration reaches a value of  $-23000 \mu\text{m}/\mu\text{s}^2$ ,
- the results obtained with the proposed model indicate that the radial residual stresses are concentrated at the coating/substrate interface, where the stress amplitude is approximately 150 MPa and it does not depend on the coating thickness,
- an increase of the coating thickness results in an increase of the radial residual stress level in the coating (reaching a maximum of 200 MPa) and slightly stress increase in the substrate,
- the computed values of the maximum deflections of the Ti/Al<sub>2</sub>O<sub>3</sub> model are in agreement with the results obtained experimentally within the admissible tolerances

The results of FEM residual stress modelling have qualitative meaning. Other residual stress measurements are planned to verify the stress magnitude in a direct way. Further investigations should be also devoted to the analysis of the residual stresses in other coating/substrate systems or systems with coatings deposited by other spraying techniques.

#### Acknowledgements

This work has been supported by the National Science Centre under the project No. N N519 652840.

#### REFERENCES

- [1] M. Kumar, H. Singh, N. Singh, Arch. Metall. Mater. **58**, 523-528 (2012).
- [2] Z. Gan, H.W. Ng, Sur. Coat. Tech. **187**, 307-319 (2004).
- [3] J. Stoks, L. Looney, Sur. Coat. Tech. **177-178**, 18-23 (2004).
- [4] M. Li, P. Christofides, Chem. Eng. Sci. **60**, 3649-3669 (2005).
- [5] J.W. Hutchinson, A.G. Evans, Sur. Coat. Tech. **149**, 179-184 (2002).
- [6] V. Luzin, K. Spencer, M.-X. Zhang, Acta Mater. **59**, 1259-1270 (2011).
- [7] C. Lyphout, P. Nyle'n, A. Manescu, T. Pirling, J. Therm. Spray. Techn. **17**(5-6), 915-923 (2008).
- [8] A. Góral, L. Lityńska-Dobrzyńska, W. Żórawski, K. Bernet, J. Wojewoda-Budka, Arch. Metall. Mater. **58**, 336-339 (2013).
- [9] D.Y. Ju, M. Nishida, T. Hanabusa, J. Mater. Process. Tech. **92-93**, 243-250 (1999).
- [10] X. Feng, Y. Huang, A.J. Rosakis, Transactions of the ASME **74**, 1276-1281 (2007).
- [11] M. Wenzelburger, M. Escribano, R. Gadow, Sur. Coat. Tech. **180-181**, 429-435 (2004).
- [12] A.M. Kamara, K. Davey, Solid and Structures **44**, 8532-8555 (2007).
- [13] M. Toparlija, F. Sen, O. Culha, E. Celik, J. Mater. Process. Tech. **190**, 26-32 (2007).
- [14] D. Golański, T. Wierzchoń, P. Biliński, J. Materials Science Letters **14**, 1499-1501 (1995).
- [15] T. Chmielewski, D. Golański, Welding Int. **1**, 1-6 (2011).
- [16] X.C. Zhang, B.S. Xu, H.D. Wang, Y.X. Wu, Materials and Design **27**, 308-315 (2006).
- [17] H.W. Ng, Z. Gan, Finite Elem. Anal. Des. **41**, 1235-1254 (2005).
- [18] A.N. Khan, J. Lu, H. Liao, Sur. Coat. Tech. **168**, 291-299 (2003).
- [19] X.C. Zhang, J. Gong, S. Tu, J. Mater. Sci. Tech. **20** (2), 149-153 (2004).
- [20] K.R. Donner, F. Gaertner, T. Klassen, J. Therm. Spray. Techn. **20** (1-2), 299-306 (2011).
- [21] T. Chmielewski, Application of kinetic energy of friction and detonation wave for metallisation of ceramics, Scientific Papers of Warsaw University of Technology. Mechanic Series **242**, 1-157 (2012), (in Polish).
- [22] C.H. Amon, R. Merz, F.B. Prinz, K.S. Schmaltz, J. Heat Transf. **118**, 164-172 (1996).
- [23] R. Boyer, G. Welsch, E. Collings, Materials Property Handbook: Titanium Alloys, ASM International, Materials Park (1994).
- [24] A. Goldsmith, T.E. Waterman, H.J. Hirchorn, Handbook of thermophysical properties of solid materials. New York (1961).
- [25] A. Mezin, Sur. Coat. Tech. **200**, 5259-5267 (2006).
- [26] V.L. Hein, F. Erdogan, International Journal of Fracture Mechanics **7**, 3, 317-330 (1971).
- [27] H. Murakawa, Y. Ueda, Transactions of JWRI **20**, 1, 109-116 (1991).